Revista Brasileira de Ensino de Física, vol. 46, e20230261 (2024)
www.scielo.br/rbef
DOI: https://doi.org/10.1590/1806-9126-RBEF-2023-0261

Drag coefficient of vertically moving popcorns

Eduardo do Carmo*[1], Marcelo Goncalves Hönnicke[1]

[1]Universidade Federal da Integração Latino-Americana, Instituto de Ciências da Vida e da Natureza, Foz do Iguaçu, PR, Brasil.

Received on September 06, 2023. Revised on January 25, 2024. Accepted on January 31, 2024.

To take the students attention in physics lectures is always a challenge. The projectile motion is not an exception. Then, study of popcorn motion can be a way to introduce and motivate the students in this subject. In this work, the popcorn flight, caused by the popping process was recorded by a cellular phone and analyzed frame by frame. Then, the drag coefficient (C_D) of vertically moving popcorns is determined and its dependency with the vertical velocity (v_y) and with the Reynolds number (Re) is explored. Our results show that C_D increases exponentially when v_y decreases. Also, C_D shows higher uncertainties when the popcorn is close to its maximum vertical trajectory. The dependency of C_D with Re shows that the popcorn flights are governed, mainly, by a laminar flow motion ($Re < 2000$).

Keywords: Drag coefficient, popcorn, tracker.

1. Introduction

The oldest ears of popcorn grains (Zea Mays L.) are dated from $\sim$ 6700–5500 calibrated years before present (cal BP) [1]. However, it is speculated that popcorn itself becomes a common food only at $\sim$ 4500–4200 cal BP [1]. Thereof, the popcorn snack have been feeding people and attracting the scientists attention mainly because the popping process. Since the popcorn producer buy the popcorn grains by weight and sell them, popped, by volume, then, to understand the popping process mechanisms in order to increase the popped popcorn grain volume is economically relevant [2] . To understand the popping process itself, different papers have been reported in the literature [3–7]. The conditions where the popcorn grain pops [3–5], the mechanical mechanism that makes the popped popcorn grain jumps and the critical temperature where the popcorn grain pops were investigated [5–7]. However, in spite of having hundreds of slow motion movies on the popcorn flights available in internet, the studies on the physics of the popcorn motion are scarce. Then, in order to introduce and motivate the students in the physics of motion, in this work we propose to study vertically moving popcorns, by analyzing, frame by frame, the popping process movie, recorded by a cellular phone.

Air resistance plays an important role in the movement of objects with small masses and relatively large cross-sectional areas (such as popcorn). From a theoretical point of view, the inclusion of air resistance in the equations of movement can turn the problem very difficult, including coupled nonlinear equations, which can be solved only by numerical methods or, through complicated algebra [8, 9]. The classical quadratic speed dependence on air resistance, which is suitable for bodies moving at higher speeds, is mediated by a drag coefficient C_D (a dimensionless quantity which encapsulates the complex dependencies on shape and flow). C_{Ds} of various objects have been explored in the literature, e.g., ping-pong ball [10], $C_D = 0.40$; pitched baseball [11], $0.31 \leq C_D \leq 0.34$; falling balls [12], $0.34 \leq C_D \leq 0.77$ and; different vehicles (bicycle, car, van and truck) [13], $0.3 \leq C_D \leq 1.49$. In all these cases, C_D was considered constant. However, C_D is velocity dependent. This dependence is explored in our experiment, which involves the vertical motion of popcorn, which is a special case of projectile motion.

2. Comments on Drag Force in Projectile Motion

Physics students are familiar with projectile motion since high school. This physics introductory content is a challenge for them because they have to deal, by the first time, with a pair of different equations that describe a unique motion. Likewise, they need to handle with some parameters to make the projectile to reach some specific point. Also, the introductory physics experiment classes is almost always approached as ideal (without air resistance). However, the effects of drag are not negligible, especially for objects with small masses and relatively large cross-sectional areas.

If we considered a model, for the drag force (F_D), that is linear in the speed, i.e., the Stokes model, then it is straightforward to solve the equations of motion. But the Stokes drag force is valid only for Reynolds numbers (Re) smaller than 1 (low speed, small size, or

*Correspondence email address: eduardo.carmo@unila.edu.br

high viscosity) [8, 9]. For example, a sphere composed of a material with the same density of water, moving in air, might have a radius smaller or equals to 4.10^{-5} m. This magnitude is not that far from the mean free path of air molecules [8, 9].

For the majority of cases, a quadratic model in speed, the Newtonian model, is assumed as a good approximation for F_D [14–17], so that:

$$F_D = \frac{1}{2}\rho A C_D v^2, \tag{1}$$

where ρ is the fluid (liquid or gas) density, A is the cross sectional area, and v is the speed. The C_D, which appears in the quadratic model, depends on many system factors and it is well described for a smooth spherical projectile [10–12]. The relation given by the equation (1) can be used in a larger range of Re ($1 \ll Re \lesssim 10^5$) [9].

Despite of the gain in different applications, the two-dimensional quadratic problem does not have an analytical solution, as recently discussed [18, 19]. The two-dimensional quadratic drag becomes to be described by a set of coupled nonlinear differential equations that are solvable only numerically [8, 9]. This explains why the Newtonian drag force appears only in one-dimensional problems and never in the general projectile motion problems of our introductory physics course.

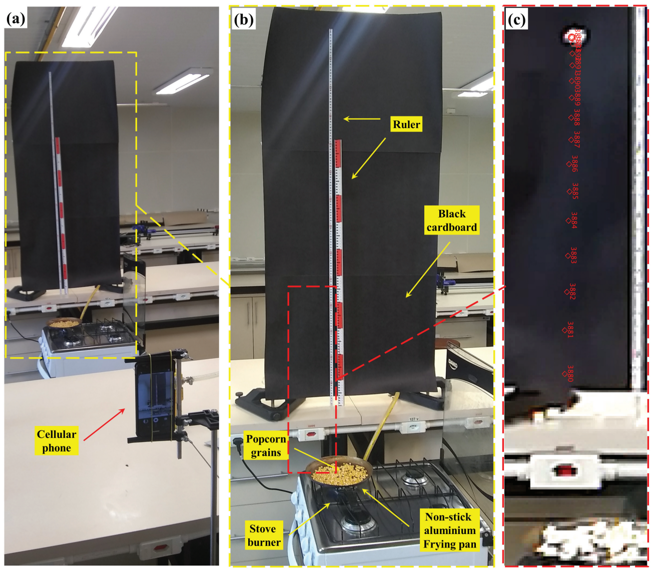

Figure 1: (a) General view of the experiment, showing where the cellular phone was set in order to record the popping process. (b) Details on the experiment for determining the drag coefficient (C_D) of vertically moving popcorns. (c) Multiframe image, mounted with the software Tracker from one of the multi-frame popcorn motion movie segmentations (popcorn flights), over a time interval of 0.56 s, i.e., 67 frames. However, only 15 frames, sort overall the full time interval, are shown.

3. Popcorn Motion and Drag Coefficient Analysis

In order to analyze the popcorn motion, which is a projectile motion an experiment (Figure 1a) with a lidless non-stick aluminum frying pan (1.5 cm height and diameter of 25 cm), a stove burner, a ruler (to calibrate, by the video frames, popcorn position), a black cardboard (as back surface to help the popcorn position measurement) and a cellular phone (Huawei P10 selfie) were used to register the popcorn motion movie (120 frames per second – fps). Three different sets, with popcorn grains amount enough to cover all the surface of the non-stick aluminum frying pan (∼500 popcorn grains per set) were prepared and considered. Soybean oil was used to cook the popcorn grains.

Note that, special care is demanded in order to minimize the parallaxes errors in video analysis experiments [20, 21]. Our experiment contains parallaxes errors especially due to the ruler (used as position reference) which was set far from the popcorn trajectory (∼30 cm, which was a safe distance to avoid collisions between the popcorns and the ruler and the back surface) and to the camera focus which was not focused in the middle of the popcorn trajectory (but it is difficult, since it is impossible to foresee any popcorn trajectory before it pops). Ideally, the ruler should be very close to the popcorn trajectory and the camera should be set as parallel as possible from the experiment plane and with the focus set in the middle of the popcorn trajectory (avoiding the trajectory borders), to avoid excessive parallaxes errors.

Most of the popcorn motion trajectories were curved. Nevertheless, we were able to select cases in which the popcorn moved straight up. Around 17 flights, overall the ∼1500 flights on the three different sets were selected (e.g., Figure 1b) and analyzed by using the software Tracker [22]. Popcorn position (y) versus time (t) data, were extracted (e.g., Figure 2). All the 17 analyzed flights have their trajectories fit with a 3rd order polynomial function by using the software Mathematica [23]. This was the best fitting function. Also, the 3rd order can be justified because the vertical acceleration (a_y), has a time variation, since the air resistance plays an important role in the popcorn motion. For the aerodynamic model considered here [14–17], the F_D is given by the equation (1). However, since we are dealing with particular case of vertical movements, v is replaced by v_y (the vertical popcorn velocity). v_y is a quadratic function, differentiated from the fitted trajectory functions (e.g., Figure 2), for each different popcorn flight.

By the 2nd Newton law, when the gravitational and F_D are the only forces acting on the popcorn, we have:

$$P + F_D = m a_y, \tag{2}$$

where $P = m \cdot g$ is the weight, m is the average popcorn mass [24] and g the gravitational acceleration. Then, by setting the equation (1) in (2):

$$-mg - \frac{1}{2}\rho A C_D v_y^2 = m a_y. \tag{3}$$

The minus signal is because the straight up popcorn movement was considered positive. Then, dividing everything by m:

$$a_y = -g - \frac{1}{2m}\rho A C_D v_y^2. \tag{4}$$

And, by taking:

$$\gamma = \frac{\rho A C_D}{2mg}, \tag{5}$$

the equation of motion becomes [15]:

$$a_y = -g(1 + \gamma v_y^2). \tag{6}$$

Then, by using the air density [25] $\rho = 1.21$ kg/m^3, the average popcorn cross sectional area, $A = 3.40 \times 10^{-4} \pm 5 \times 10^{-6}$ m^2 [24], the average popcorn mass, $m = 2.13 \times 10^{-4} \pm 3 \times 10^{-6}$ kg [24], the v_y and a_y functions, differentiated from each different fitted trajectory function (3$^{\text{rd}}$ order polynomial function – e.g., Figure 2), it is possible to solve the equation (4) in order to get the different $C_D s$:

$$C_D = -\frac{2m(a_y + g)}{\rho A v_y^2}. \tag{7}$$

Few of the calculated $C_D s$ versus v_y are shown in Figure 3. The velocity dependency is showed up. C_D increases exponentially when v_y decreases. This behavior is the same for any different popcorn flight. Also, by the results one can see that for higher $v_y s$, i.e., when the different popcorn flights start, the $C_D s$ show lower uncertainties (percent error ∼10%, calculated by the differences between the maximum and minimum C_D values, at higher $v_y s$, shown in Figure 3). While, for lower $v_y s$, i.e., when the popcorn is close to its maximum vertical trajectory, the $C_D s$ show higher uncertainties (percent error ∼60%, calculated by the differences between the maximum and minimum C_D values, at lower $v_y s$, shown in Figure 3). This increased uncertainty is expected, since at the maximum height there is no movement and should not have a drag.

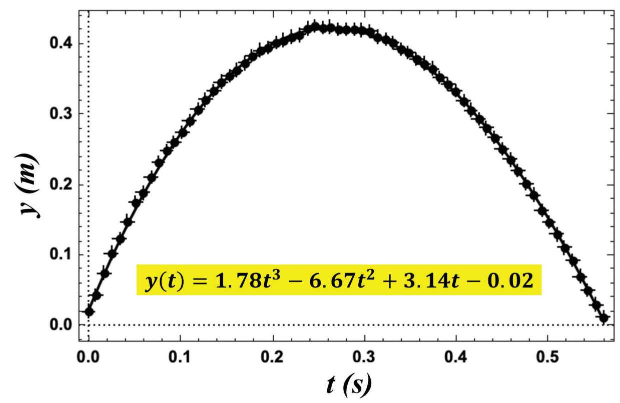

Figure 2: (a) Position (y) versus time (t) data, acquired with software Tracker, for the popcorn flight shown in Figure 1(b). The data follow a 3$^{\text{rd}}$ order polynomial function, as specified. For all the 17 analyzed flights, the data, even being different, show the same behavior. The error bars in y and t are also indicated (appears as crosses in the figure).

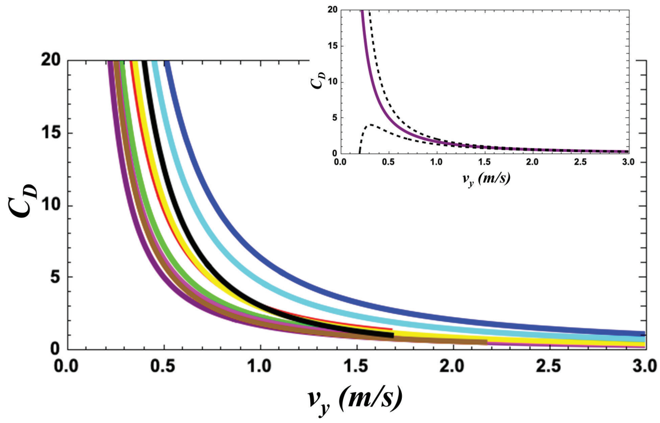

Figure 3: Drag coefficient (C_D) versus vertical popcorn velocity (v_y) for 10 different flights. C_D increases exponentially when v_y decreases, has lower uncertainties for higher $v_y s$ (percent error ∼10%) and higher uncertainties for lower $v_y s$ (in general, percent error ∼60%, diverging when $v_y \to 0$). The result for the popcorn flight shown in Figure 1(b) is shown in dark purple and emphasized in the inset with the error bars indicated by the dashed lines.

Still taking use of the v_y functions it is possible to explore the dependency of C_D with Re (Figure 4). The Re is defined by [26]:

$$Re = \frac{\rho v_y L}{\eta}, \tag{8}$$

where L is the characteristic length and η is the air kinematic viscosity (1.84.10^{-5} Pa.s) [23]. L was given by popcorn average diameter, i.e.:

$$L = 2\sqrt{\frac{A}{\pi}}. \tag{9}$$

As well as for the velocity, the C_D increases exponentially when the Re decreases. Note that, except in the beginning, where the $v_y s$ are higher and the flow can be considered transitional between laminar and turbulent flow motion ($2000 < Re < 3500$) [27], the popcorn flights are governed, mainly, by a laminar flow motion ($Re < 2000$) [27]. Note that a deeper analysis should take into account the air heat produced by the cooking process in the frying pan. However this was not taken into account.

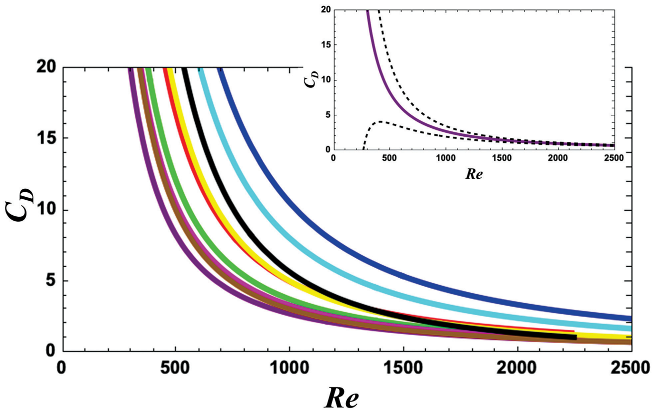

Figure 4: Drag coefficient (C_D) versus Reynolds number (*Re*) for 10 different flights. Again, the result for the popcorn flight shown in Figure 1(b) is shown in dark purple. C_D increases exponentially when *Re* decreases. The result for the popcorn flight shown in Figure 1(b) is shown in dark purple and emphasized in the inset with the error bars indicated by the dashed lines. The error increases when *Re* decreases showing a divergence when $Re \to 0$. The popcorn flights are governed, mainly, by a laminar flow motion ($Re < 2000$).

4. Summary and Conclusion

The drag coefficient (C_D) for vertically moving popcorns was explored. Our results show that C_D, which is velocity dependent, increases exponentially when the vertical velocity (v_y) decreases. Also, one can see that, for higher $v_y s$, i,e., when the popcorn motion starts, the C_D, show lower uncertainty (percent error $\sim 10\%$), while, for lower $v_y s$, when the popcorn is close to its maximum vertical trajectory, the C_D show higher uncertainties (percent error $\sim 60\%$). This increased uncertainty is expected, since at the maximum height there is no movement and the drag should be zero. At last, the dependency of C_D with the Reynolds number (*Re*) was also explored. It was possible to check that C_D increases exponentially when the *Re* decreases and the popcorn flights are governed, mainly, by a laminar flow motion ($Re < 2000$).

Acknowledgments

The authors acknowledge Mr. Wagner Ferreira for the help in providing the stove used in this experiment.

References

[1] A. Grobman, D. Bonavia, T.D. Dillehay, D.R. Piperno, J. Iriarte and I. Holst, PNAS **109**, 1755 (2012).
[2] B.L. Weaver and A.E. Thompson, *White hulless popcorn: fifteen generations of selection for improved popping expansion* (University of Illinois, Illinois, 1957).
[3] W.J. da Silva, B.C. Vidal, M.E.Q. Martins, H. Vargas, C. Pereira, M. Zerbetto and L.C.M. Miranda, Nature **362**, 417 (1993).
[4] S. Gökmen, J. Food Eng. **65**, 357 (2004).
[5] D.D. Metzger, K.H. Hsu, K.E. Ziegler and C.J. Bern, Cereal Chem. **66**, 247 (1989).
[6] E. Virot and A. Ponomarenko, J. R. Soc. Interface **12**, 20141247 (2015).
[7] R.C. Hoseney, K. Zeleznak and A. Abdelrahman, J. Cereal Sci. **1**, 43 (1983).
[8] J.L. Bradshaw, Am. J. Phys. **91**, 258 (2023).
[9] G.W. Parker, Am. J. Phys. **45**, 606 (1977).
[10] Y. Zhang, Y. Zhao, R. Xiong, Y. Wang, J. Wang and J. Chu, IEEE International Conference on Robotics & Automation (ICRA), 4108 (2014).
[11] D. Kagan, Phys. Teacher **52**, 278 (2014).
[12] D. Cross and C. Lindsey, Phys. Teacher **52**, 169 (2014).
[13] D. Fahsl and P. Vogt, Phys. Teacher **56**, 324 (2018).
[14] M. Nagurka, Int. J. Engng. Ed. **19**, 623 (2003).
[15] P. Timmerman and J.P. van der Weele, Am. J. Phys. **67**, 538 (1999).
[16] R.G. Lunnon, Proc. R. Soc. Lond. A **110**, 302 (1926).
[17] L.D. Landau and E.M. Lifsshitz, *Fluid Dynamics* (Pergamon Press, Oxford, 1987).
[18] F.L. da Silveira, Rev. Bras. Ens. Fís. **45**, e20230060 (2023).
[19] V.B. Mendrot and A.S. de Castro, Rev. Bras. Ens. Fís. **45**, e20230186 (2023).
[20] J. Stephens, M. Bostjancic and T. Koskulitz, Phys. Teach. **57**, 193 (2019).
[21] T. Martin, K. Frisch and J. Zwart, Phys. Teach. **58**, 195 (2020).
[22] D. Brown, *Tracker – video analysis and modeling tool*, available in: https://physlets.org/tracker/.
[23] Wolfram Research, *Mathematica 13.3*, available in: https://www.wolfram.com/mathematica/.
[24] E. do Carmo and M.G. Hönnicke, Rev. Bras. Ens. Fís. **43**, e20210115 (2021).
[25] D. Halliday, R. Resnick and J. Walker, *Fundamentals of Physics* (John Wiley & Sons, New Jersey, 1994) 4 ed.
[26] N. Rott, Annu. Rev. Fluid Mech. **22**, 1 (1990).
[27] U.S. DEPARTMENT OF ENERGY, *DOE Fundamentals Handbook: Thermodynamics, Heat Transfer, and Fluid Flow*, available in: https://www.steamtablesonline.com/pdf/Thermodynamics-Volume3.pdf.